

## 3D Two-Fluid Braginskii Simulations of the Large Plasma Device

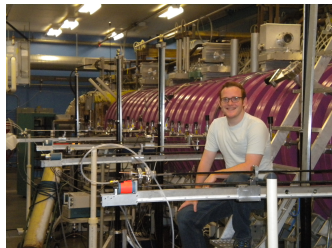
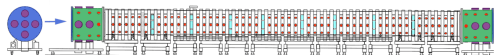
Dustin Fisher<sup>†</sup>, Barrett Rogers<sup>†</sup>, Giovanni Rossi<sup>\*</sup>, Danny Guice<sup>\*</sup>

<sup>†</sup>Department of Physics and Astronomy, Dartmouth College, Hanover, New Hampshire 03755, USA

<sup>\*</sup>Department of Physics and Astronomy, University of California, Los Angeles, California 90095, USA

### Conclusions:

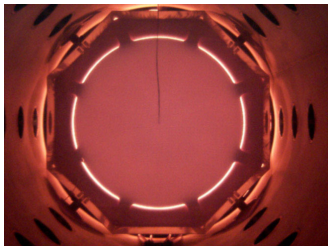
- ★ 3D global 2-fluid simulations show good agreement with data from LAPD in the low-bias parameter regime explored so far.
- ★ KH turbulence at relatively large scales is the dominant driver of cross-field transport in the low-bias simulations.
- ★ Biased simulations are currently under study.



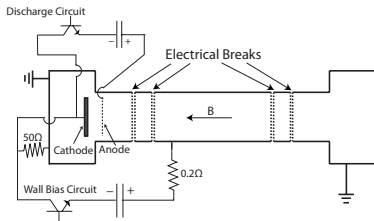
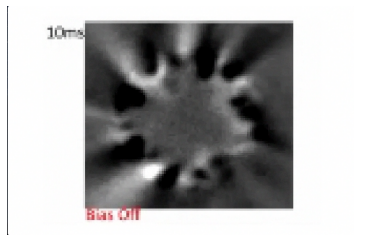
The work presented here builds upon an initial numerical study [Rogers and Ricci, *Phys. Rev. Lett.*, **104**, 2010] of LAPD [Gekelman et al., *Rev. Sci. Instrum.*, **62**, 1991] using the Global Braginskii Solver code (GBS) [Ricci et al., *Plasma Phys. Control. Fusion*, **54**, 2012].

## LAPD Primer for a Nominal He Plasma

- Plasma 17 m in length, 30 cm in radius
- Machine diameter  $\simeq 1\text{m}$
- $n \sim 2 \times 10^{12} \text{ cm}^{-3}$
- Pulsed at 1 Hz for  $\sim 10\text{ms}$
- Axial magnetic field  $\sim 1\text{kG}$
- $T_e \sim 6\text{eV}$  and  $T_i \sim 0.5\text{eV}$
- Ion sound gyroradius,  $\rho_s \sim 1.4\text{cm}$
- Plasma  $\beta \sim 10^{-4}$



<http://plasma.physics.ucla.edu/pages/gallery.html> (BaPSF)



T.A. Carter and J.E. Maggs, *Physics of Plasmas*, 16 (2009)



# Standard Bohm Sheath B.C.'s at the End Walls

$$V_{\parallel i} = \pm c_s \quad (1)$$

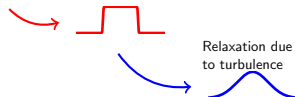
$$V_{\parallel e} = \pm c_s \exp([\Lambda - e\{\phi_{\text{plasma}} - \phi_{\text{wall}}\}/T_e]) \quad (2)$$

with

$$c_s = \sqrt{T_{e0}/m_i}; \quad \Lambda = \ln \sqrt{m_i/(2\pi m_e)} \sim 3 \quad (3)$$

The B.C.'s on the outflows of ions and electrons to the end walls lead to an approximate global balance  $V_{\parallel i} \sim V_{\parallel e}$ , or

$$\phi_{\text{plasma}} \sim \Lambda T_e \quad (4)$$





The code evolves a set of electrostatic two-fluid drift-reduced Braginskii equations assuming  $T_i \ll T_e$ :

$$\frac{dn}{dt} = -\frac{\partial (nV_{\parallel e})}{\partial z} + \mathcal{D}_n(n) + S_n \quad (5)$$

$$\begin{aligned} \frac{dT_e}{dt} = & -V_{\parallel e} \frac{\partial T_e}{\partial z} + \frac{2}{3} \frac{T_e}{en} 0.71 \frac{\partial j_{\parallel}}{\partial z} \\ & - \frac{2}{3} T_e \frac{\partial V_{\parallel e}}{\partial z} + \mathcal{D}_{T_e}^{\parallel}(T_e) + \mathcal{D}_{T_e}(T_e) + S_T \end{aligned} \quad (6)$$

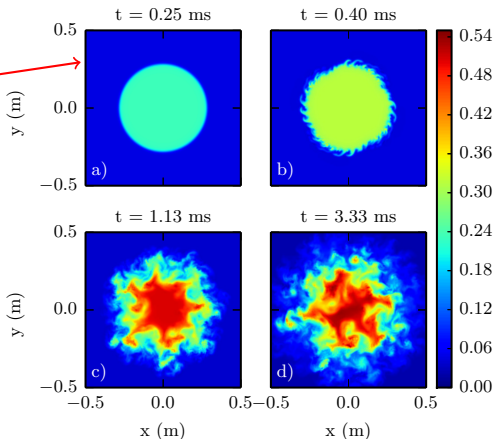
$$\begin{aligned} m_e \frac{dV_{\parallel e}}{dt} = & -m_e V_{\parallel e} \frac{\partial V_{\parallel e}}{\partial z} + \frac{4}{3} \frac{\eta_{0e}}{n} \frac{\partial^2 V_{\parallel e}}{\partial z^2} + \frac{ej_{\parallel}}{\sigma_{\parallel}} \\ & + e \frac{\partial \phi}{\partial z} - \frac{T_e}{n} \frac{\partial n}{\partial z} - 1.71 \frac{\partial T_e}{\partial z} \end{aligned} \quad (7)$$

$$m_i \frac{dV_{\parallel i}}{dt} = -m_i V_{\parallel i} \left( \frac{\partial V_{\parallel i}}{\partial z} \right) + \frac{4}{3} \frac{\eta_{0i}}{n} \frac{\partial^2 V_{\parallel i}}{\partial z^2} - \frac{1}{n} \frac{\partial p_e}{\partial z} \quad (8)$$

$$\frac{d\omega}{dt} = -V_{\parallel i} \frac{\partial \omega}{\partial z} + \frac{m_i \Omega_{ci}^2}{e^2 n} \frac{\partial j_{\parallel}}{\partial z} - \nu_{in} \omega + S_{\omega} \quad (9)$$

# Evolution of Turbulence and Transport

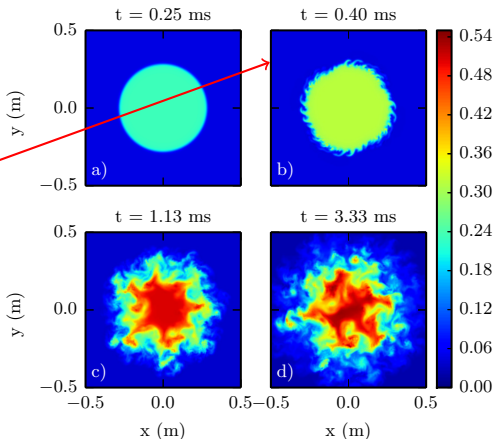
- Starting top-hat shaped density source.
- Onset of drift waves with  $k_{\theta} \rho_s \sim 0.5$ ,  $k_{\parallel} L_{eq} \sim 1$ .
- Onset of KH from sheared flow with  $k_{\parallel} \sim 0$ .
- Steady-state region where turbulence has reached saturation.



Plots show mid-plane cuts perpendicular to B.

# Evolution of Turbulence and Transport

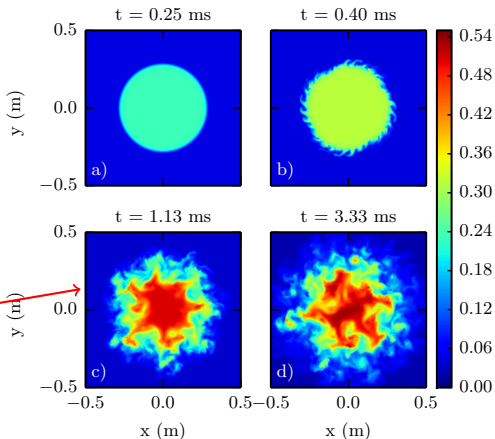
- Starting top-hat shaped density source.
- Onset of drift waves with  $k_{\theta} \rho_s \sim 0.5$ ,  $k_{\parallel} L_{eq} \sim 1$ .
- Onset of KH from sheared flow with  $k_{\parallel} \sim 0$ .
- Steady-state region where turbulence has reached saturation.



Plots show mid-plane cuts perpendicular to B.

# Evolution of Turbulence and Transport

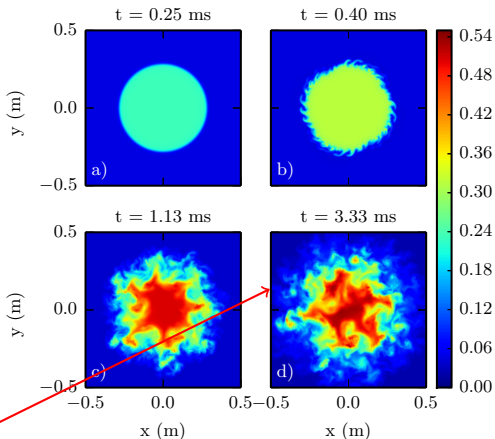
- Starting top-hat shaped density source.
- Onset of drift waves with  $k_{\theta} \rho_s \sim 0.5$ ,  $k_{\parallel} L_{eq} \sim 1$ .
- Onset of KH from sheared flow with  $k_{\parallel} \sim 0$ .
- Steady-state region where turbulence has reached saturation.



Plots show mid-plane cuts perpendicular to B.

# Evolution of Turbulence and Transport

- Starting top-hat shaped density source.
- Onset of drift waves with  $k_{\theta} \rho_s \sim 0.5$ ,  $k_{\parallel} L_{eq} \sim 1$ .
- Onset of KH from sheared flow with  $k_{\parallel} \sim 0$ .
- Steady-state region where turbulence has reached saturation.

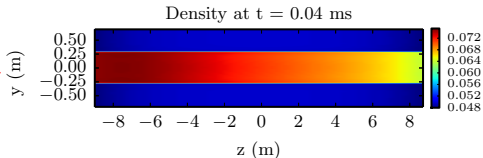


Plots show mid-plane cuts perpendicular to B.

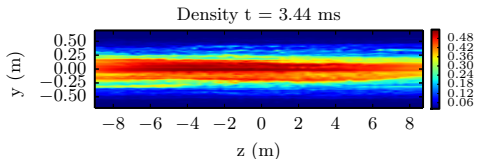


# Fluctuations Predominantly $k_{\parallel} = 0$

Top Starting exponential source dependence.



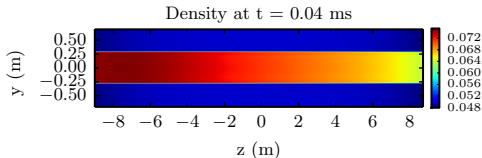
Bottom Profile modified by turbulence.



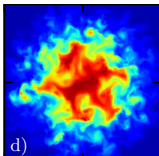
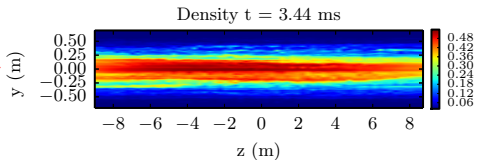
Plots show mid-plane cuts parallel to B.

# Fluctuations Predominantly $k_{\parallel} = 0$

Top Starting exponential source dependence.



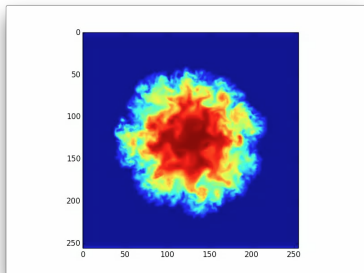
Bottom Profile modified by turbulence.

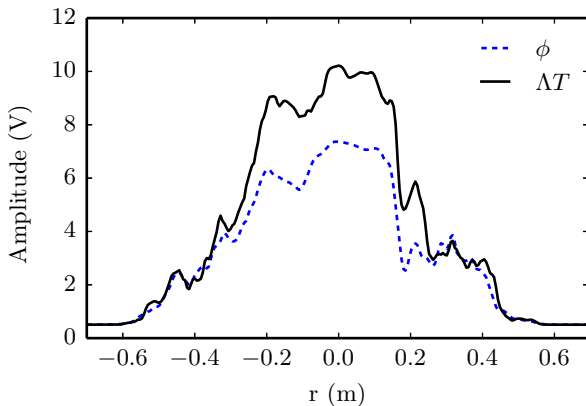


Plots show mid-plane cuts parallel to B.

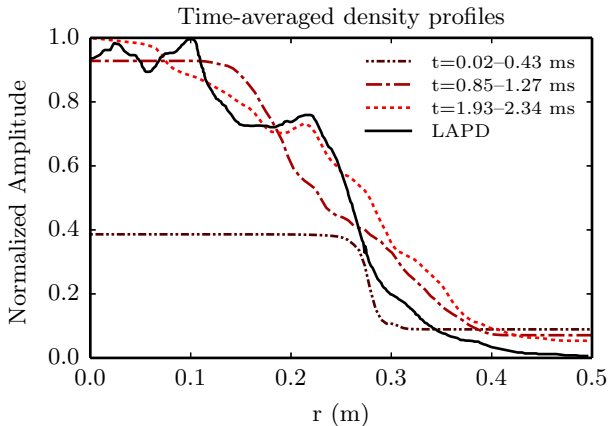


# Low Bias with Intrinsic Rotation due to Sheath B.C.'s





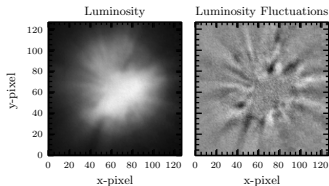
Potential profile that forms self-consistently from the temperature profile and the boundary sheath conditions. Here  $\Lambda = 3$ .



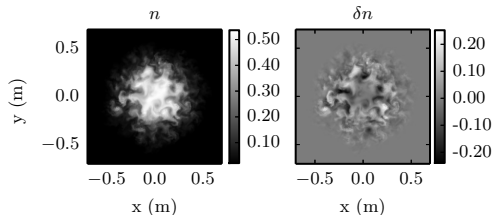
# CCD Camera Comparisons

Luminosity data from a Phantom camera looking down the length of the LAPD.

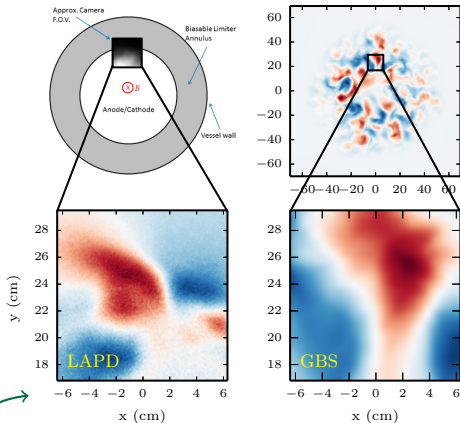
## LAPD



## Simulation

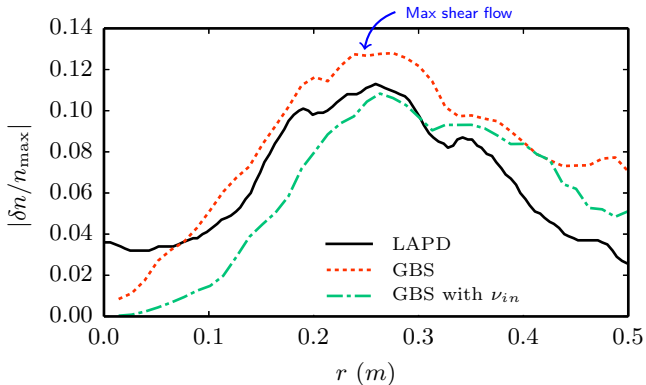


- Presence of density holes inside the cathode edge and blobs outside.
- Scale size of visible density fluctuations comparable to simulations.



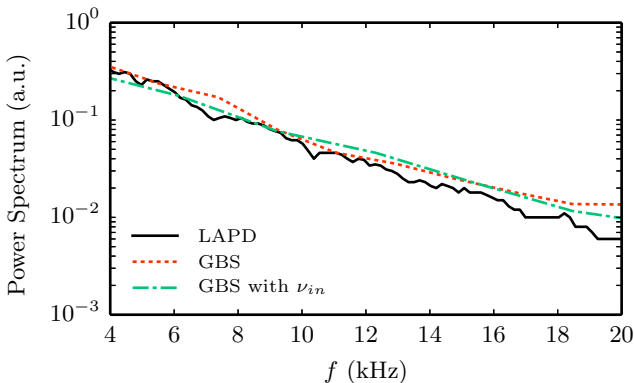
**LAPD** Filtered, mean-subtracted luminosity data from LAPD using a periscopic mirror arrangement.

**Simulation** Line-averaged density fluctuations from GBS zoomed to the same window size as the CCD data.

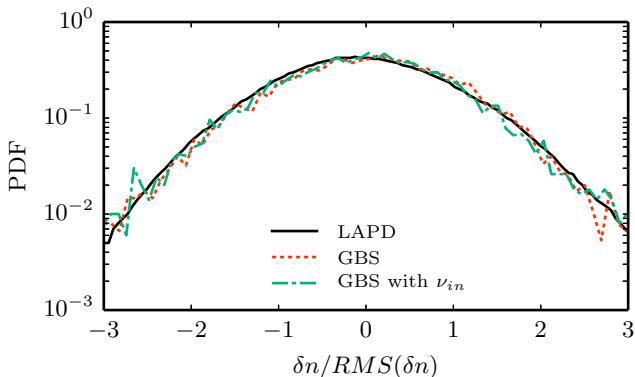


- Peak fluctuations occur where the shear flow is greatest.
- Theorized  $\nu_{in}$  leads to modest stabilizing effect on KH modes.





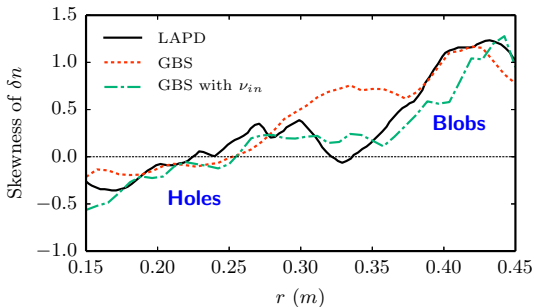
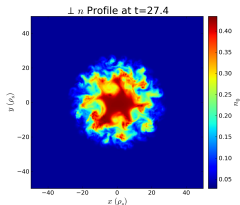
- Exponential spectra consistent with intermittent turbulent structures (Pace, Shi, Maggs, Morales, and Carter, *Phys. Rev. Lett.*, 101, 2008).



Probability distribution function of density fluctuations averaged over the interval  $22 \text{ cm} \leq r \leq 28 \text{ cm}$ .

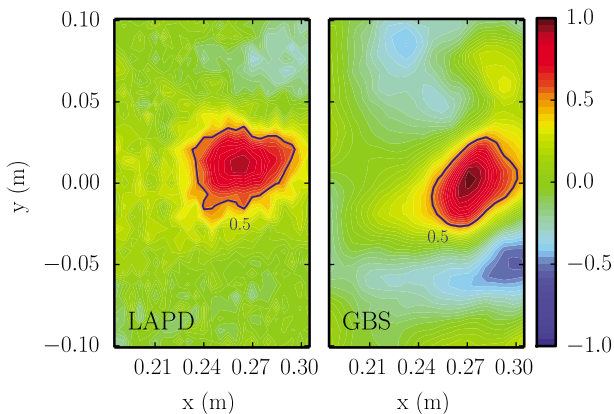
Intermittent turbulence can be spotted by its effect on the third standardized moment of the distribution function known as the skewness:

$$\text{Skewness} = \frac{\frac{1}{N} \sum_N \delta n^3}{\left(\frac{1}{N} \sum_N \delta n^2\right)^{3/2}}$$

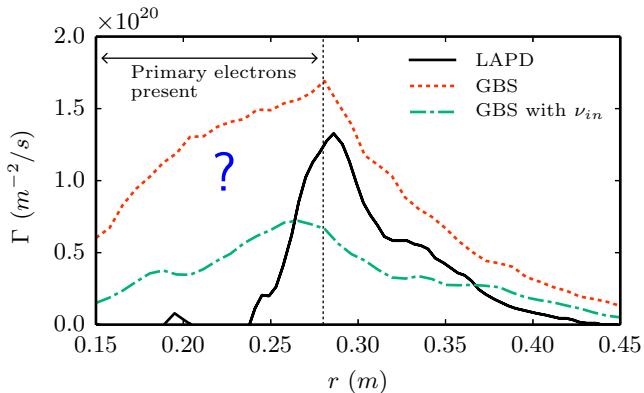


Negative skewness indicates a left tail in the PDF which is linked to the presence of density **holes**. Positive skewness indicates the PDF is skewed to the right by a density tail which may signal the presence of density **blobs**.

2D cross-field correlation function of the density fluctuations referenced to a point near the cathode. edge



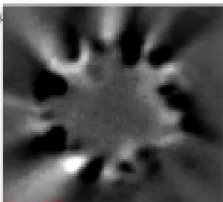
A solid line marks the correlation at 0.5 below the maximum value to give a correlation length of  $\simeq 5.5\text{cm}$  consistent with KH scale lengths.



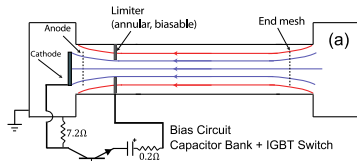
- Data inside cathode edge unreliable due to fast electrons.
- Theorized  $\nu_{in}$  value drops transport by a factor of 2.

## Biasing in LAPD

10ms



Bias Off

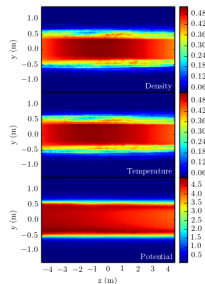
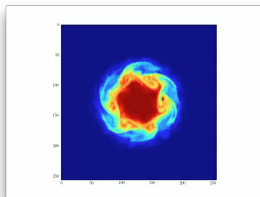
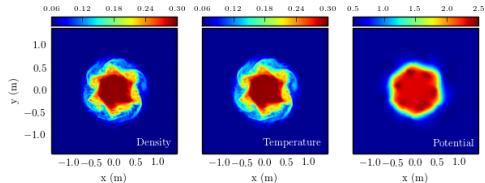
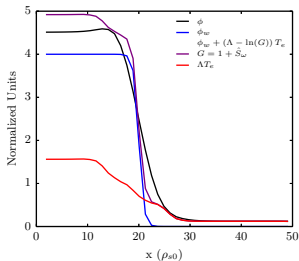


[Schaffner et. al., *Phys. Plasmas*, **20**, 2013]

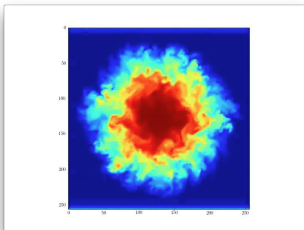
- Original biasing of LAPD was done by biasing the chamber walls relative to the cathode [Maggs, Carter, and Taylor, *Phys. Plasmas*, **14**, 2007].
- Recently, a biasable limiter was used for continuous variation of the shear flow by David Schaffner and colleagues.

# Increasing the Shear Flow

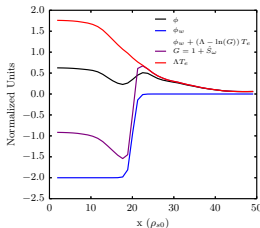
## LAPD Biased Run $m \sim 6$ mode



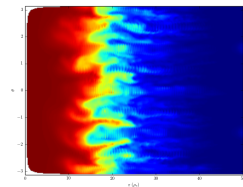
# Reducing/Nulling/Reversing the Shear Flow



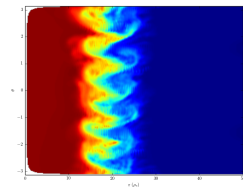
Current work focuses on completely nulling the shear flow to explore the effects drift wave modes have on turbulence and transport without KH from shear flow.



Density with Decreased Shear Flow



Density with Increased Shear Flow







## Conclusions

- Overall good agreement between the simulations and LAPD data.
- Sheath boundary conditions lead to  $\phi_{\text{plasma}} \sim \Lambda T_e + \phi_{\text{wall}}$ .
- Large shear flow destabilizes KH which appears to be the dominant driver of turbulence and transport in the unbiased case. Pressure gradients also destabilize small scale drift waves.
- Ion-neutral collisions have a modest stabilizing effect on the KH modes, and reduce the radial transport by approximately a factor of two for the theoretically predicated ion-neutral collision frequency.
- Biasing can increase, null, or reverse shear flow in the plasma. The physics of these biased runs are currently being studied.

Our next step is to null the shear flow to study driftwaves in the absence of KH driven shear flows.



To add a source to the vorticity equation, one assumes a small electron source term representing the primary electronics coming from the hot cathode.

$$\frac{\partial n_i}{\partial t} + \nabla \cdot [n (\mathbf{v}_{E \times B} + \mathbf{v}_{di} + \mathbf{v}_{pol} + v_{\parallel i} \mathbf{b})] = S_i \quad (10)$$

$$\frac{\partial n_e}{\partial t} + \nabla \cdot [n (\mathbf{v}_{E \times B} + \mathbf{v}_{de} + v_{\parallel e} \mathbf{b})] = S_e + S_{e,f} \quad (11)$$

Subtracting (11) from (10) and assuming quasi-neutrality gives a current continuity equation with a small source term that can be physically thought of as relating to the discharge current each time the plasma is pulsed.

$$\nabla \cdot [n (\mathbf{v}_{di} - \mathbf{v}_{de})] + \nabla \cdot (n \mathbf{v}_{pol}) + \frac{\partial}{\partial z} \left( \frac{j_{\parallel}}{e} \right) = -S_{e,f} \quad (12)$$



Using the Boussinesq approximation and neglecting magnetic curvature terms

$$\nabla \cdot (n\mathbf{v}_{\text{pol}}) \simeq -\frac{nc}{B\omega_{ci}} \frac{d}{dt} (\nabla_{\perp}^2 \phi) \quad (13)$$

the vorticity equation with  $\omega = \nabla_{\perp}^2 \phi$  can be written

$$\frac{d\omega}{dt} = \frac{m_i \omega_{ci}^2}{en} \left[ \nabla \cdot (n(\mathbf{v}_{di} - \mathbf{v}_{de})) + \frac{\partial}{\partial z} \left( \frac{j_{\parallel}}{e} \right) \right] + S_\omega \quad (14)$$



The Pedersen conductivity can be written as

$$\sigma_1 = \sigma_0 \frac{(1 + \kappa) \nu_e^2}{(1 + \kappa)^2 \nu_e^2 + \omega_{ce}^2} \quad (15)$$

where

$$\sigma_0 = \frac{ne^2}{m_e \nu_e} \quad (16)$$

$$\kappa = \frac{\omega_{ce} \omega_{ci}}{\nu_e \nu_{in}} \quad (17)$$

$$\nu_e = \nu_{en} + \nu_{ei} \quad (18)$$

and the collision frequencies for the electrons with neutrals,  $\nu_{en}$ , the electrons with ions,  $\nu_{ei}$ , and the ions with neutrals,  $\nu_{in}$  are all known from theory or experiment.



In the limit where  $\nu_{in}/\omega_{ci} \ll 1$  (valid for LAPD estimates of  $\nu_{in}/\omega_{ci} \sim 2 \times 10^{-3}$ ) the Pedersen conductivity term can be written as

$$\sigma_1 = \frac{ne^2 \nu_{in}}{m_i \omega_{ci}^2} \quad (19)$$

Ohm's law dictates that  $\mathbf{J}_\perp = -\sigma_1 \nabla \phi$  so that the perpendicular component of current in the current continuity equation becomes:

$$\nabla \cdot \mathbf{J}_\perp = \nabla \cdot (-\sigma_1 \nabla \phi) \quad (20)$$

$$= - \left( \frac{ne^2 \nu_{in}}{m_i \omega_{ci}^2} \right) \omega \quad (21)$$

where it's assumed that  $\sigma_1$  is not spatially dependent as estimated for LAPD [Maggs, Carter, and Taylor, *Phys. Plasmas*, **14**, 2007].



To prevent a buildup of charge in the plasma and maintain quasi-neutrality

$$J_{\parallel\text{cathode}} = J_{\parallel w1} + J_{\parallel w2} \quad (22)$$

where  $J_{\parallel\text{cathode}}$  is the discharge current into the source and  $J_{\parallel w1, w2}$  are the currents out of the near and far walls. Balancing these terms, Eq. (1) and Eq. (2) can be written

$$\hat{j} \equiv \frac{J_{\parallel\text{cathode}}}{qn_{se}c_{se}} = 2 - \exp\left(\Lambda - \frac{e}{T_e}(\phi_{se} - \phi_{w1})\right) \times \left(1 + \exp\left(\frac{e}{T_e}(\phi_{w2} - \phi_{w1})\right)\right) \quad (23)$$

where  $n_{se}$  is the plasma density at the sheath edge,  $c_{se}$  is the sound speed at the sheath edge at which ions are assumed to enter,  $\phi_{se}$  is the plasma potential at the sheath edge, and  $\phi_{w1}$  and  $\phi_{w2}$  are the near and far wall potentials.



When  $\phi_{w1} = \phi_{w2}$  the exponential factor on the far RHS goes to unity. When  $\phi_{w1} > \phi_{w2}$  the exponential becomes negligible and vanishes. Solving for the plasma potential at the sheath edge one can show

$$\phi_{se} - \phi_{w1} = \frac{T_e}{e} \left\{ \Lambda - \ln \left[ \frac{1}{f} (2 - \hat{J}) \right] \right\} \quad (24)$$

where  $f = 1$  when  $\phi_{w1} > \phi_{w2}$  and  $f = 2$  when  $\phi_{w1} = \phi_{w2}$  and  $\hat{J} < 0$  since it's modeling an electron beam. Thus a vorticity source,  $S_\omega$  which acts as a source of current in the current continuity equation, also effectively shifts the Bohm sheath factor to a lower value when setting the plasma potential.



A modest correction to this calculated potential can likewise be made with the inclusion of ion-neutral collisions. Thus in solving the vorticity equation for a perturbed potential  $\phi = \phi_0 + \phi_1$ , with  $\phi_1 \ll \phi_0$ ,

$$e\phi = \Lambda' T_e \quad (25)$$

where

$$\Lambda' = \Lambda - \ln(G) \quad (26)$$

and

$$G \sim \left( 1 + \frac{S_\omega}{c_{se}} - \frac{\nu_{in}}{c_{se}} \nabla_\perp^2 \phi_0 \right). \quad (27)$$